OPEN

Creep rupture as a non-homogeneous Poissonian process

Zsuzsa Danku & Ferenc Kun

Department of Theoretical Physics, University of Debrecen, P.O. Box 5, H-4010 Debrecen, Hungary.

Creep rupture of heterogeneous materials occurring under constant sub-critical external loads is responsible for the collapse of engineering constructions and for natural catastrophes. Acoustic monitoring of crackling bursts provides microscopic insight into the failure process. Based on a fiber bundle model, we show that the accelerating bursting activity when approaching failure can be described by the Omori law. For long range load redistribution the time series of bursts proved to be a non-homogeneous Poissonian process with power law distributed burst sizes and waiting times. We demonstrate that limitations of experiments such as finite detection threshold and time resolution have striking effects on the characteristic exponents, which have to be taken into account when comparing model calculations with experiments. Recording events solely within the Omori time to failure the size distribution of bursts has a crossover to a lower exponent which is promising for forecasting the imminent catastrophic failure.

Materials subject to a constant external load below their fracture strength typically exhibit a time dependent response and fail in a finite time. Such creep rupture phenomena have an enormous technological importance and human impact since they are responsible for the collapse of engineering constructions and they lie at the core of natural catastrophes such as landslides, snow and stone avalanches and earthquakes[1–11]. The acoustic waves generated by the nucleation and propagation of cracks allow for the monitoring of the failure process on the meso- and micro scales. Crackling noise is usually characterized by the integrated statistics accumulating all the events of the time series up to failure[2–14]. Experiments revealed that the probability distribution of the energy of crackling bursts and of the interoccurrence times have power law functional form, which are considered to be the fingerprint of correlations in the microscopic breaking dynamics[1–14]. The value of the exponents measured on different types of heterogenous materials show a surprisingly large scatter between 1 and 2 which has not been captured by theoretical studies[1–10]. The approach to failure is usually characterized on the macroscale by the strain rate which proved to have a power law divergence as a function of time to failure[1,5,6,14].

Here we take a different strategy and investigate the details of the crackling time series in order to understand how the creeping system evolves towards catastrophic failure. We consider a generic fiber bundle model[16–20] (FBM) of damage enhanced creep rupture which successfully reproduces measured creep behaviour of heterogeneous materials both on the micro and macro scales (Methods)[21,22]. In the model under a constant subcritical external load the fibers break due to two physical mechanisms: immediate breaking occurs when the load of fibers exceeds the local failure strength. Time dependence emerges such that intact fibers accumulate damage which results in failure in a finite time. The separation of time scales of slow damaging and of immediate breaking together with the load redistribution following failure events lead to a highly complex time evolution where slowly proceeding damage sequences trigger bursts of immediate breakings[21,22]. An example of the time series of bursts can be seen in Fig. 1 where the increasing burst size Δ and the decreasing waiting time T between consecutive events clearly mark the acceleration of the system towards failure. As a novel approach to creep we focus on the evolution of the rate of bursts and show that the temporal occurrence of crackling events and the power law statistics of waiting times can fully be described based on non-homogeneous Poissonian processes without assuming correlations of bursts. Our investigation unveils that limitations of measuring devices in experiments have astonishing effects on the outcomes of crackling noise analysis which can explain the strong scatter of measured critical exponents of crackling noise in creep, and the discrepancy between experimental findings and theoretical approaches. Studying how the time series evolves when approaching the catastrophe we address the possibility of forecasting the imminent failure. The importance of the results goes beyond fracture phenomena and catastrophic failures, recently the human activity has been found to exhibit similar bursty character where analogous problems of the evolution of time series and waiting time statistics occur[23–25].
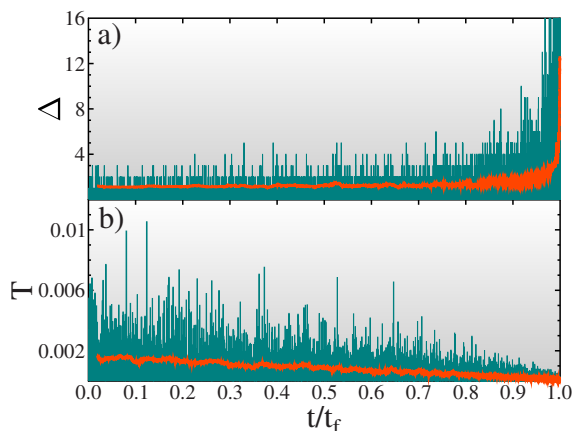
Figure 1 | Time series of bursts in a bundle of $N = 100000$ fibers at a load $\sigma_0/\sigma_c = 0.05$: the size of bursts Δ (a) and waiting times T between consecutive events (b) are presented as function of time t of their occurrence normalized by the lifetime t_f of the system. The red lines represent the moving average of Δ and T. The increasing average burst size and decreasing average waiting time indicate the acceleration of the system towards failure.

Results

Bursts of immediate breakings triggered by damage sequences are analogous to acoustic outbreaks in loaded specimens. However, damage breakings cannot be recorded by experimental means they determine the waiting time T between consecutive bursts. The competition of the two failure modes has the consequence that the system drives itself towards failure under a constant subcritical external load $\sigma_0 < \sigma_c$. The global acceleration of the dynamics that can be observed in Fig. 1 is the consequence of the increasing load on the intact part of the system due to subsequent load redistributions, while the fluctuations of the burst size Δ and waiting time T emerge due to the quenched heterogeneity of fibers' strength in qualitative agreement with experiments[1–13].

In order to quantify how the accelerating dynamics appears on the microscale we determined the rate of bursts $n(t)$ as a function of the distance from the critical point $t_f - t$. Figure 2(a) shows that at the beginning of the creep process the event rate monotonically increases having a power law functional form. Approaching catastrophic failure $n(t)$ saturates and converges to a constant. The most remarkable result is that the functional form of $n(t)$ can be described by the modified Omori law[26,27]

$$n(t) = \frac{A}{\left[1 + (t_f - t)/c\right]^p}, \qquad (1)$$

where A is the saturation rate or productivity at catastrophic failure, c denotes the characteristic time scale, and p is the Omori exponent. Perfect agreement can be observed in Fig. 2(a) between the simulated data and the analytic form of equation (1). In the case of earthquakes, the Omori law describes the decay rate of aftershocks following major earthquakes[26,27]. For creep rupture we observe the inverse process: considering the macroscopic failure as the main shock, the breaking bursts are foreshocks whose increasing rate is described by the (inverse) Omori law.

As a crucial point, our approach makes it posssible to clarify how the characteristic time scale c of the Omori law emerges: Figure 2(b) illustrates that due to the increasing load on intact fibers shorter and shorter damage sequences are sufficient to trigger bursts. However, this acceleration is limited such that for $t_f - t < c$ the average length of damage sequences $\langle \Delta_d \rangle(t)$ saturates between 1 and 2. The origin of this high susceptibility is that the load of intact fibers $\sigma_s(t)$ gradually increases to its quasi-static critical value σ_s^c (see Fig. 2(b))[16–22]. Hence, the Omori time scale c is determined by the condition $\sigma_s(t_f - t = c) \approx \sigma_s^c$, where σ_s^c can be obtained from the quasi-static constitutive equation of FBMs[16–22]. Note that the condition $\langle \Delta_d \rangle = 1$ marks the point of instability where the avalanche cannot stop anymore and it becomes catastrophic.

Figure 2(a) also demonstrates that the saturation rate A does not depend on the external load σ_0, however, the characteristic time scale c linearly increases $c \sim \sigma_0$, indicating that at higher load saturation sets on earlier. Our simulations revealed that the Omori exponent is $p = 1$, it does not depend on any details of the damage law[21,22] such as the γ exponent and the disorder distributions until the load redistribution is long ranged.

The event rate $n(t)$ is practically the inverse of the average waiting time between events occurring at time t. More detailed characterization is provided by the probability distribution of waiting times $P(T)$ which is presented in Fig. 3 corresponding to the system of Fig. 2. Along the distributions two characteristic time scales can be identified: for waiting times below a threshold $T < T_l$, the distributions have constant values, while in the limit of large waiting times $T > T_u$ a rapidly decreasing exponential form is obtained.

For the intermediate regime $T_l < T < T_u$ the waiting time distributions exhibit a power law behavior

$$P(T) \sim T^{-z}, \qquad (2)$$

where the exponent proved to be universal $z = 1$. Increasing the external load σ_0 the upper cutoff T_u decreases, however, the lower characteristic time T_l is independent of σ_0. Since the temporal occurrence of events is determined by the global increase of the breaking probability due to the increasing load on intact fibers, the above results suggest that the time evolution of crackling noise of heterogeneous materials undergoing creep rupture can be described as a
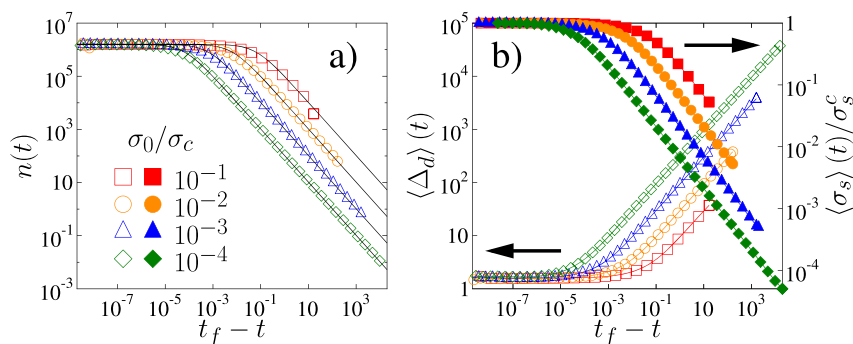

Figure 2 | (a) Event rate n as a function of time to failure $t_f - t$ for several different load values. The continuous lines represent fits with the Omori law equation (1). (b) Average size of damage sequences $\langle \Delta_d \rangle$ and average load of single fibers σ_s normalized by its quasi-static critical value σ_s^c as function of time to failure.
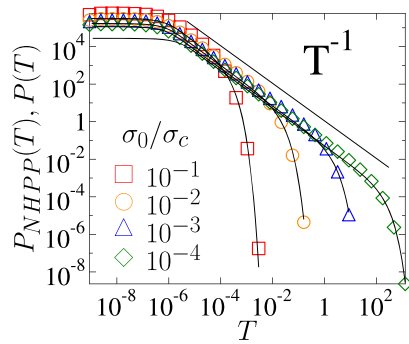
Figure 3 | Probability distribution of waiting times P(T) between consecutive bursts. The numerical results (symbols) are perfectly described by the analytic prediction $P_{NHPP}(T)$ of equation (3) (continuous lines).

non-homogeneous Poissonian process (NHPP). For NHPP the waiting time distribution of a series of N_Δ events with duration t_f can be obtained analytically from the event rate as[28,29]

$$P_{NHPP}(T) = \frac{1}{N_\Delta} \int_0^{t_f - T} n(s)n(s+T)e^{-\int_s^{s+T} n(u)du}ds + n(t)e^{-\int_0^T n(s)ds}. \quad (3)$$

To verify the consistency of the NHPP picture for our creeping system, first we fitted the event rate functions by the Omori law determining the value of the parameters A, c, and p. Then the analytic form equation (1) of $n(t)$ with the numerical parameters was plugged into equation (3) and the integral was calculated numerically taking into account the load dependent lifetime $t_f(\sigma_0)$ of the sample[21,22], as well. In Fig. 3 an excellent agreement can be observed between the waiting time distributions obtained from the simulations $P(T)$ and the analytic prediction $P_{NHPP}(T)$ of equation (3). An important consequence of the above results is that the lower cutoff T_l of $P(T)$ can be obtained from the saturation event rate $T_l = 1/A$, which does not depend on the external load. The upper cutoff T_u is determined by the other time scales as $T_u = \frac{1}{A}\left(\frac{t_f}{c}\right)^p$. Inserting the Basquin law of creep life $t_f \propto \sigma_0^{-\gamma}$ reproduced by our model[21,22] and the linear load dependence of c it follows that the upper cutoff T_u scales with the external load as $T_u \sim \sigma_0^{-(1+\gamma)}$. The results show that details of the damage process control the global time scale of rupture, however, they do not affect the Omori and waiting time exponents. Power law distributions of interoccurrence times in fracture phenomena are usually considered to be the fingerprint of correlations between consecutive events[1-14]. Our analysis revealed that for creep phenomena this is not necessarily true, the global acceleration of a heterogeneous system can lead to power law distributed inter-event times without any local correlations.
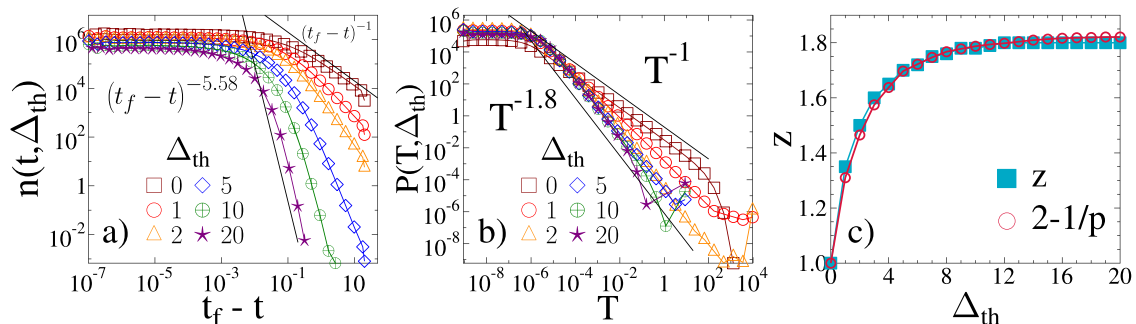
The comparison of theoretical results to the experimental findings and different types of measurements to each other can be problematic because in laboratory experiments the time series of bursts is never complete: small size bursts generate only low amplitude signals which may fall in the range of background noise[1-11]. Devices also have a finite time resolution resulting in a deadtime of detection, during which bursts generated at different positions in space cannot be distinguished from each other[1-11,15,30]. Incompleteness of the time series, especially in field observations, may also be caused by the fact that recording does not start exactly at the time when the load was set. Hence, the beginning of the time series is missing and the measurement is more focused on the vicinity of the failure point where intensive crackling occurs[1-4,32-34].

In order to capture the effect of the detection threshold of the measuring equipment in the data evaluation, we introduced a threshold value Δ_{th} for the size of bursts Δ, i.e. bursts with size $\Delta \leq \Delta_{th}$ are ignored in the time series. Since the size of bursts increases when approaching global rupture (see Fig. 1), the detection threshold removes events typically at the beginning of the time series decreasing the rate of events in this regime. It can be observed in Fig. 4(a) that as Δ_{th} increases the functional form of the event rate $n(t, \Delta_{th})$ remains nearly the same described by the Omori law equation (1), however, the exponent p monotonically increases with the threshold value Δ_{th}. For the corresponding waiting time distributions $P(T, \Delta_{th})$ in Fig. 4(b), the exponent z of the power law regime also increases with increasing Δ_{th}, however, the NHPP nature of the event series is preserved at any values of Δ_{th}. For NHPPs the two exponents z and p have the simple relation[28]

$$z(\Delta_{th}) = 2 - 1/p(\Delta_{th}), \quad (4)$$

which holds with a high accuracy in our system for the numerically determined exponents at any values of Δ_{th} (see Fig. 4(c)). It is important to emphasize that the exponents increase due to the non-stationary nature of creep rupture: the simultaneous increase of the rate and size of events towards failure has the consequence that the finite detection threshold mainly affects the beginning of the time series resulting in a few long waiting times up to the first bigger bursts. Their statistics is characterized by a peak or small bump in Fig. 4(b), while the rest of waiting times have a steeper power law distribution. The results demonstrate that the detection threshold has a dramatic effect on the outcomes of the analysis of crackling time series, just varying Δ_{th} practically any values can be obtained for the waiting time exponent z between 1 and 2.

The finite time resolution t_d of the detectors has the consequence that bursts pile up, i.e. since bursts cannot be distinguished within the duration t_d, the size of bursts sums up giving rise to larger event sizes in the time series. The effect of the deadtime is captured in the data evaluation such that if an avalanche of size Δ_i occurred at time t_i, all those avalanches which appeared in the interval $t_i < t < t_t + t_d$ are added to Δ_i. In Fig. 5(a) at zero deadtime $t_d = 0$ where all avalanches

Figure 4 | Event rates (a) and waiting time distributions (b) at different detection thresholds Δ_{th}. (c) Comparison of the exponent $z(\Delta_{th})$ of the waiting time distributions obtained numerically with the NHPP prediction equation (4).
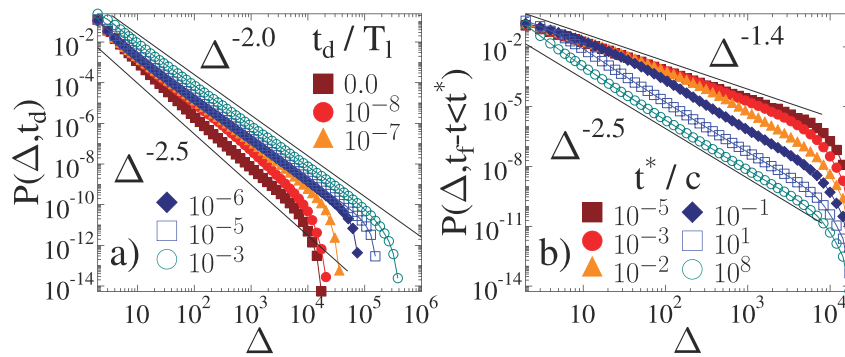
Figure 5 | (a) Burst size distributions at $\sigma_0/\sigma_c = 0.001$ for different values of the deadtime t_d. A crossover is observed from a power law of exponent $\tau = 2.5$ to a lower value $\tau_d = 2.0$ (b) Considering events solely close to failure $P(\Delta, t_f - t < t^*)$ shows a crossover from the exponent 2.5 to 1.4.

are distinguished the size distribution $P(\Delta, t_d = 0)$ has a power law form

$$P(\Delta, t_d = 0) \sim \Delta^{-\tau} \qquad (5)$$

followed by an exponential cutoff. The value of the exponent $\tau = 2.5$ is equal to the usual mean field burst exponent of FBMs[16–22]. As t_d increases the pile up of bursts promotes large events while the small ones get suppressed. Due to the acceleration of the failure process pile-up gets dominating in the vicinity of macroscopic failure, hence, in Fig. 5(a) the value of t_d is compared to T_l of the waiting time distribution. As a consequence, the waiting time distributions hardly change, however, the burst size distribution $P(\Delta, t_d)$ has a crossover to a power law of a significantly lower exponent $\tau_d = 2.0$ showing the higher frequency of large events in the statistics. In Fig. 5(a) pile up becomes dominating already at $t_d/T_l \approx 0.001$, which shows the importance of the results for real experiments.

Recently, laboratory experiments on earth materials have revealed that the b-value, i.e. the exponent of the probability distribution of the energy of the time series of acoustic events of rupture cascades decreases in the vicinity of failure[31–34]. To investigate the possibility of an analogous phenomenon in creep rupture, we constrained the data evaluation to events occurring in a time interval of duration t^* preceding macroscopic failure and determined the probability distribution $P(\Delta, t_f - t < t^*)$. It can be observed in Fig. 5(b) that approaching macroscopic rupture $t^* < c$, where the largest avalanches are triggered, the burst size distribution $P(\Delta, t_f - t < t^*)$ exhibits a crossover: at a characteristic burst size Δ_c the exponent of $P(\Delta, t_f - t < t^*)$ has a striking change from $\tau = 2.5$ to a surprisingly low value $\tau \approx 1.4$. The value of Δ_c extends to the largest avalanche as $t^* < c$ decreases. The crossover is accompanied by the change of the waiting time distribution, as well: Since in the regime $t^* < c$ the event rate is constant, the power law regime of $P(\Delta, t_f - t < t^*)$ disappears and the distribution turns to a pure exponential as it is expected for homogeneous (constant event rate) Poissonian processes[29].

Discussion

Acoustic outbreaks generated by nucleating and propagating cracks provide the main source of information on the microscopic temporal dynamics of creep rupture. For the understanding of acoustic monitoring data of engineering constructions and of field measurements on steep slopes or rock walls in mountains requires the application of statistical physics. Our analysis showed that time-to-failure power laws of macroscopic quantities such as creep rate commonly observed in experiments are accompanied by the emergence of Omori type acceleration of the bursting activity on the microscale. The origin of the Omori time scale is that the aging system drives itself to a critical state where a few breakings are sufficient to trigger extended bursts. The Omori law is known to describe the relaxation of the rate of aftershocks following major earthquakes[26,27], and it has

also been confirmed for foreshocks when observed[32]. Our results suggest the interpretation that acoustic bursts in creep behave like foreshocks of the imminent catastrophe.

Our investigations unveiled that the evolving time series of crackling events is the result of an underlying non-homogeneous Poissonian process. It has the striking consequence that observing power law distributed waiting times in fracture may not imply the presence of dynamic correlations, up to a large extent it can be caused by the global acceleration of the system. We showed that special care should be taken when comparing results of model calculations to measurements on crackling noise, since the deadtime of devices and the finite background noise to signal ratio can even affect the measured value of critical exponents. Varying solely the detection threshold of events, for the distribution of waiting times any exponents can be obtained between 1 and 2 covering the range of experimental results[1–15]. Due to the finite deadtime of electronics bursts pile up which gives rise to a crossover to a lower exponent of the size distribution of bursts. Recently, avalanches have been identified with a high spacial resolution along a propagating crack front using optical imaging techniques[15,30]. Considering global avalanches in the same experiment integrates bursts along the front, giving rise to a significantly lower exponent in agreement with our predictions[15,30].

Components of engineering constructions are mainly subject to creep loads[3], and creep rupture often lies at the core of natural catastrophes such as landslides, snow and stone avalanches, as well[31–34]. We demonstrated that restricting the measurement to the close vicinity of ultimate failure, the size distribution of bursts exhibits a crossover to a significantly lower exponent, which is accompanied by the change of the functional form of the waiting time distribution. Since the crossover is controlled by the time scale of the Omori law these results can be exploited for forecasting the imminent catastrophic failure event.

Here we focused on the case of long range load redistribution following failure events. When the load sharing is localized the spatial correlation of failure events leads to the emergence of a propagating crack front. The load accumulated along the crack front gives rise to an overall acceleration of the failure process again with a non-homogeneous Poissonian character. However, at short time scales correlated clusters of events may arise inside the time series. The results imply the interesting question to clarify when studying burst time series under creep whether there is anything in the dynamics beyond non-homogeneous Poissonian processes.

Methods

We use a generic fiber bundle model[16–20] of the creep rupture of heterogeneous materials which has succesfully reproduced measured creep behavior[21,22]. The sample is discretized in terms of a bundle of N parallel fibers having a brittle response with identical Young modulus E. The bundle is subject to a constant external load σ_0 below the fracture strength σ_c of the system. It is a crucial element of the model that the fibers break due to two physical mechanisms: immediate breaking occurs when the

4

local load σ on fibers exceeds their fracture strength $\sigma_{th}^i, i = 1, \ldots, N$. Time dependence is introduced such that those fibers, which remained intact, undergo an aging process accumulating damage $c(t)$[21,22]. The rate of damage accumulation $\Delta c(t)$ is assumed to have a power law dependence on the local load $\sigma(t)$ of fibers $\Delta c(t) = a\sigma(t)^\gamma \Delta t$, where a is a constant and the exponent γ controls the time scale of the accumulation process. Fibers can tolerate only a finite amount of damage so that when the total damage $c(t)$ accumulated up to time t exceeds a local damage threshold c_{th}^i the fiber breaks. The two breaking thresholds σ_{th}^i and $c_{th}^i, i = 1, \ldots, N$ of fibers are independent random variables which are for simplicity uniformly distributed between 0 and 1. After each breaking event the load dropped by the broken fiber is equally redistributed over the remaining intact ones[21,22].

The separation of time scales of slow damage and of immediate breaking leads to the emergence of a bursty evolution of the system: damaging fibers break slowly one-by-one, gradually increasing the load on the remaining intact fibers. After a certain number of damage breakings the load increment becomes sufficient to induce the immediate breaking of a fiber which in turn triggers an entire burst of breakings. As a consequence, the time evolution of creep rupture occurs as a series of bursts corresponding to the nucleation and propagation of cracks, separated by silent periods of slow damaging. The size of burst Δ is defined by the number of fibers breaking in a correlated trail, while the waiting time T between consecutive events is the duration of the damage sequence of Δ_d breakings which triggers the next event. Macroscopic failure occurs in the form of a catastrophic avalanche at time t_f which defines the lifetime of the system[21,22]. Our model reproduces the Basquin law of creep life, i.e. the lifetime t_f decreases as a power law of the external load $t_f \propto \sigma_0^{-\gamma}$, where the exponent coincides with the exponent of damage accumulation γ[21,22].

Computer simulations were carried out in our FBM with $N = 10^7$ fibers averaging over 1000 samples for each parameter set except for Fig. 1 where intensionallly a small bundle of $N = 10^5$ fibers were considered. The exponent γ of the damage law mainly sets the global time scale of the evolution, hence, the simulation results are presented only for $\gamma = 1$. Other parameters of the model are fixed as $E = 1$ and $a = 1$[21,22].

1. Nechad, H., Helmstetter, A., El Guerjouma, R. & Sornette, D. Creep ruptures in heterogeneous materials. *Phys. Rev. Lett.* **94**, 045501 (2005).
2. Petri, A., Paparo, G., Vespignani, A., Alippi, A. & Costantini, M. Experimental Evidence for Critical Dynamics in Microfracturing Processes. *Phys. Rev. Lett.* **73**, 3423 (1994).
3. Niccolini, G., Carpinteri, A., Lacidogna, G. & Manuello, A. Acoustic emission monitoring of the syracuse athena temple: Scale invariance in the timing of ruptures. *Phys. Rev. Lett.* **106**, 108503 (2011).
4. Maes, C., van Moffaert, A., Frederix, H. & Strauven, H. Criticality in creep experiments on cellular glass. *Phys. Rev. B* **57**, 4987–4990 (1998).
5. Garcimartin, A., Guarino, A., Bellon, L. & Ciliberto, S. Statistical properties of fracture precursors. *Phys. Rev. Lett.* **79**, 3202 (1997).
6. Guarino, A., Garcimartin, A. & Ciliberto, S. An Experimental Test of the Critical Behaviour of Fracture Precursors. *Eur. Phys. J. B* **6**, 13–24 (1998).
7. Rosti, J., Koivisto, J. & Alava, M. J. Statistics of acoustic emission in paper fracture: precursors and criticality. *J. Stat. Mech.* **2010**, P02016 (2010).
8. Miksic, A., Koivisto, J. & Alava, M. Statistical properties of low cycle fatigue in paper. *J. Stat. Mech.* **2011**, P05002 (2011).
9. Santucci, S., Cortet, P., Deschanel, S., Vanel, L. & Ciliberto, S. Subcritical crack growth in fibrous materials. *Europhys. Lett.* **74**, 595–599 (2006).
10. Ramos, O., Cortet, P.-P., Ciliberto, S. & Vanel, L. Experimental Study of the Effect of Disorder on Subcritical Crack Growth Dynamics. *Phys. Rev. Lett.* **110**, 165506 (2013).
11. Deschanel, S., Vanel, L., Vigier, G., Godin, N. & Ciliberto, S. Statistical properties of microcracking in polyurethane foams under tensile test, influence of temperature and density. *Int. J. Fract.* **140**, 87–98 (2006).
12. Sethna, J. P., Dahmen, K. A. & Meyers, C. R. Crackling noise. *Nature* **410**, 242–250 (2001).
13. Dahmen, K. A., Ben-Zion, Y. & Uhl, J. T. A simple analytic theory for the statistics of avalanches in sheared granular materials. *Nat. Phys.* **7**, 554–557 (2011).
14. Sornette, D. Predictability of catastrophic events: Material rupture, earthquakes, turbulence, financial crashes, and human birth. *Proc. Nat. Acad. Sci. USA* **99**, 2522–2529 (2002).
15. Bonamy, D., Santucci, S. & Ponson, L. Crackling dynamics in material failure as the signature of a self-organized dynamic phase transition. *Phys. Rev. Lett.* **101**, 045501 (2008).
16. Moreno, Y., Gomez, J. B. & Pacheco, A. F. Fracture and Second-Order Phase Transitions. *Phys. Rev. Lett.* **85**, 2865 (2000).
17. Pradhan, S., Hansen, A. & Hemmer, P. C. Crossover behavior in burst avalanches: Signature of imminent failure. *Phys. Rev. Lett.* **95**, 125501 (2005).
18. Pradhan, S., Hansen, A. & Chakrabarti, B. K. Failure processes in elastic fiber bundles. *Rev. Mod. Phys.* **82**, 499–555 (2010).
19. Hidalgo, R. C., Moreno, Y., Kun, F. & Herrmann, H. J. Fracture model with variable range of interaction. *Phys. Rev. E* **65**, 046148 (2002).
20. Yoshioka, N., Kun, F. & Ito, N. Size Scaling and Bursting Activity in Thermally Activated Breakdown of Fiber Bundles. *Phys. Rev. Lett.* **101**, 145502 (2008).
21. Kun, F., Carmona, H. A., Andrade, Jr., J. S. & Herrmann, H. J. Universality behind basquin's law of fatigue. *Phys. Rev. Lett.* **100**, 094301 (2008).
22. Kun, F., Halász, Z., Andrade, J. S. & Herrmann, H. J. Crackling noise in sub-critical fracture of heterogeneous materials. *J. Stat. Mech.* **2009**(01), P01021 (2009).
23. Barabási, A.-L. The origin of bursts and heavy tails in human dynamics. *Nature* **435**, 207–211 (2005).
24. Karsai, M., Kaski, K., Barabási, A.-L. & Kertész, J. Universal features of correlated bursty behaviour. *Sci. Rep.* **2**, 397; DOI:10.1038/srep00397 (2012).
25. Malmgren, R. D., Stouffer, D. B., Motter, A. E. & Amaral, L. A. N. A poissonian explanation for heavy tails in e-mail communication. *Proc. Nat. Acad. Sci. USA* **105**, 18153–18158 (2008).
26. Utsu, T. A statistical study of the occurrence of aftershocks. *Geophys. Mag.* **30**, 521–605 (1961).
27. Utsu, T., Ogata, Y. & Matsu'ura, R. S. The centenary of the Omori formula for a decay law of aftershock activity. *J. Phys. Earth* **43**, 1–33 (1995).
28. Shcherbakov, R., Yakovlev, G., Turcotte, D. L. & Rundle, J. B. Model for the distribution of aftershock interoccurrence times. *Phys. Rev. Lett.* **95**, 218501 (2005).
29. Daley, D. J. & Vere-Jones, D. An Introduction to the Theory of Point Processes. Springer (New York), 2002.
30. Laurson, L., Santucci, S. & Zapperi, S. Avalanches and clusters in planar crack front propagation. *Phys. Rev. E* **81**, 046116 (2010).
31. Amitrano, D., Gruber, S. & Girard, L. Evidence of frost-cracking inferred from acoustic emissions in a high-alpine rock-wall. *Earth Planet. Sci. Lett.* **341**, 86–93 (2012).
32. McGuire, J. J., Boettcher, M. S. & Jordan, T. H. Foreshock sequences and short-term earthquake predictability on east pacific rise transform faults. *Nature* **434**, 457–461 (2005).
33. Sammonds, P. R., Meredith, P. G. & Main, I. G. Role of pore fluids in the generation of seismic precursors to shear fracture. *Nature* **359**, 228–230 (1992).
34. Amitrano, D. Variability in the power-law distributions of rupture events, How and why does b-value change. *Eur. Phys. J. B, Special Topics* **205**, 199–215 (2012).

Acknowledgments

Author contributions

Zs. D. performed computer simulations and evaluated the numerical data. F. K. designed the research, evaluated numerical data and wrote the manuscript.

Additional information